Functional differences between neonatal and adult fibroblasts and keratinocytes: Donor age affects epithelial-mesenchymal crosstalk *in vitro*

ROSANA MATEU[1], VERONIKA ŽIVICOVÁ[1,2], ELIŠKA DROBNÁ KREJČÍ[1], MILOŠ GRIM[1], HYNEK STRNAD[3], ČESTMÍR VLČEK[3], MICHAL KOLÁŘ[3], LUKÁŠ LACINA[1,4], PETER GÁL[5-7], JIŘÍ BORSKÝ[8], KAREL SMETANA JR[1,9] and BARBORA DVOŘÁNKOVÁ[1,9]

[1]Institute of Anatomy and [2]Department of Otorhinolaryngology and Head and Neck Surgery, First Faculty of Medicine, Charles University; [3]Institute of Molecular Genetics, Academy of Sciences of the Czech Republic vvi; [4]Department of Dermatology and Venereology, Charles University, First Faculty of Medicine, Prague, Czech Republic; [5]Department for Biomedical Research, East-Slovak Institute of Cardiovascular Diseases; [6]Department of Pharmacology, Faculty of Medicine, Pavol Jozef Šafárik University, Košice; [7]Department of Pharmacognosy and Botany, Faculty of Pharmacy, Commenius University, Bratislava, Slovak Republic; [8]Department of ENT, Second Faculty of Medicine, Charles University in Prague and Motol University Hospital, Prague; [9]BIOCEV, Vestec, Czech Republic

Received April 13, 2016; Accepted July 25, 2016

DOI: 10.3892/ijmm.2016.2706

Abstract. Clinical evidence suggests that healing is faster and almost scarless at an early neonatal age in comparison with that in adults. In this study, the phenotypes of neonatal and adult dermal fibroblasts and keratinocytes (nestin, smooth muscle actin, keratin types 8, 14 and 19, and fibronectin) were compared. Furthermore, functional assays (proliferation, migration, scratch wound closure) including mutual epithelial-mesenchymal interactions were also performed to complete the series of experiments. Positivity for nestin and α smooth muscle actin was higher in neonatal fibroblasts (NFs) when compared with their adult counterparts (adult fibroblasts; AFs). Although the proliferation of NFs and AFs was similar, they significantly differed in their migration potential. The keratinocyte experiments revealed small, poorly differentiated cells (positive for keratins 8, 14 and 19) in primary cultures isolated from neonatal tissues. Moreover, the neonatal keratinocytes exhibited significantly faster rates of healing the experimentally induced *in vitro* defects in comparison with adult cells. Notably, the epithelial/mesenchymal interaction studies showed that NFs in co-culture with adult keratinocytes significantly stimulated the adult epithelial cells to acquire the phenotype of small, non-confluent cells expressing markers of poor differentiation. These results indicate the important differences between neonatal and adult cells that may be associated with improved wound healing during the early neonatal period.

Correspondence to: Dr Barbora Dvořánková, Institute of Anatomy, First Faculty of Medicine, Charles University, U Nemocnice 3, 128 00 Prague, Czech Republic
E-mail: barbora.dvorankova@lf1.cuni.cz

Key words: newborn, nestin, keratin, repair, regeneration, scar, fibrosis, extracellular matrix

Introduction

It has been well documented that prenatal skin wounds heal rapidly and without scar formation. Although the molecular and cellular network underlying this phenomenon is not yet fully understood, increasing evidence suggests that this phenomenon may be associated with an attenuated prenatal immune response (1-3). Anecdotal clinical evidence has suggested that an attenuated immune response can still be present at a very early postnatal period of life, and it may be associated with excellent wound healing as seen during digital distal phalanx regeneration in mice and infants (4). Furthermore, cleft lip reconstructive surgery performed during the first postnatal week ensures a quick and almost scarless healing process (5). Primary human keratinocytes and fibroblasts isolated from residual tissues following cleft lip surgery have provided a unique opportunity to compare the most important structural components participating in tissue repair and regeneration, in newborns and older children (6).

Epithelial-mesenchymal interactions (EMIs) are well known to play important roles during the course of many physiological and pathological processes including the repair of skin and mucous membranes. For instance, EMIs are responsible for the morphogenesis of acral type epidermis (7). Moreover, EMIs initiate a sequence of events leading to several developmental steps determining the fate of epithelial and mesenchymal cells and resulting in the development of skin appendages such as hair follicles and nails (8). The development and maintenance of tissue architecture depends upon

a chain of EMIs that are controlled by several factors such as bone morphogenetic protein (BMP)-3, Sonic hedgehog and members of the WNT family (8,9). Mesenchymal cells can even determine the type of arising appendages as was demonstrated in 1963 in a series of elegant experiments using avian embryos (10). These data suggest that EMIs are important for the formation of cutaneous appendages and underscore the formative potential of dermal fibroblasts.

Fibroblasts and endothelial cells are principal cellular components of granulation tissue. It is important that sufficient wound granulation occurs to replace lost tissue before re-epithelisation from wound edges and hair follicles takes place (11). Activated fibroblasts start to synthesize components of the extracellular matrix (ECM) and organize them into mechanically supportive structures. They are also frequently transformed to α smooth muscle actin (αSMA)-expressing cells, the myofibroblasts (MFs) (12-14). MFs generate remarkable contractile force leading to wound contraction and they also produce various bioactive growth factors, cytokines and chemokines (13). On the other hand, they also release multiple proteases responsible for dynamic remodeling and turnover of ECM components. The presence of activated fibroblasts and/or MFs is not strictly restricted to wound healing. They are also a hallmark of tumors. In this scenario, cancer-associated fibroblasts (CAFs) also significantly influence the biological properties of tumors including local aggressivity and the formation of distant metastases (15). Compared with normal fibroblasts, CAFs differ significantly in the expression of almost 600 genes as determined by whole genome transcriptional analysis (16). Furthermore, CAFs are able to influence the differentiation pattern of normal keratinocytes including the induction of epithelial-mesenchymal transition *in vitro* (17,18). Factors produced by activated fibroblasts, namely insulin-like growth factor (IGF)-2, BMP-4, interleukin (IL)-6, IL-8, chemokine (C-X-C motif) ligand 1 (CXCL1), fibroblast growth factor 7 (FGF-7), leptin, nerve growth factor (NGF) and transforming growth factor-β (TGF-β), can influence the epithelial and other cell types at the wound and cancer site, respectively (16,19,20). Using a similar repertoire of signaling cascades, the final biological outcome is remarkably different in wounds and tumors.

It is evident that the age-dependent clinical presentation of scars following cleft lip reconstructive surgery calls for a better understanding of the basic biological processes underlying the fibrotic and regenerative capacities of higher organisms. Hence, the present study is focused on a functional and phenotypic comparison of fibroblasts and keratinocytes isolated from newborns and adults. To complete the series of experiments, we further studied the EMIs of these cells in matching and non-matching combinations *in vitro*.

Materials and methods

Isolation of cells. Residual skin from cleft lip reconstructive surgery in 3 newborns and aesthetic surgery waste material in 3 adults was used to isolate keratinocytes and fibroblasts. These samples were obtained at the Ear, Nose and Throat (ENT) Department of the Second Faculty of Medicine and the Department of Plastic Surgery of the Third Faculty of Medicine, at Charles University in Prague. All samples were acquired under Local Ethics Committee approval together with explicit written informed consent from the patients or their legal representatives in the case of minors. The processing of skin samples and the isolation of cell populations was described by Krejčí *et al* (6). Fibroblasts were cultured in Dulbecco's modified Eagle's medium (DMEM) supplemented with antibiotics (penicillin 100 U/ml and streptomycin 100 μg/ml) and 10% fetal bovine serum (FBS) (all from Biochrom GmbH, Berlin, Germany) and cultured at 37˚C and 5% CO_2 in a humidified incubator. Keratinocytes were cultured on mitomycin C-treated (Sigma-Aldrich, Prague, Czech Republic) 3T3 feeder cells in keratinocyte medium DMEM + F12 3:1 with 10% FBS, supplemented with 0.4 μg/ml hydrocortisone, 10^{-10} M cholera toxin, 10 ng/ml epidermal growth factor (all from Sigma-Aldrich) and 0.12 U/ml insulin Actrapid (Novo Nordisk, Bagsværd, Denmark) under the same conditions.

Multipotency assessment of neonatal fibroblasts (NFs) and adult fibroblasts (AFs). The adipogenic, chondrogenic and osteogenic potential of NFs and AFs was tested using a commercial Human Mesenchymal Stem Cell Functional Identification kit (R&D Systems, Minneapolis, MN, USA). Briefly, 1,000 cells/cm^2 on fibronectin-coated coverslips were applied and cultured for 3 consecutive days in DMEM supplemented with 5% FBS. The cells were cultured for a total of three weeks according to the manufacturer's instructions. The differentiation status of the tested cells was examined using antibodies provided in the kit.

Migration of fibroblasts. NFs and AFs were also used to perform a migration assay. Briefly, the cells were inoculated in 6-well plates (Corning, Rochester, NY, USA). Each well contained 7 isolated 10 μl-drops in a regular geometrical arrangement providing a constant distance between neighboring drops at baseline in all cases. Each inoculum contained 5,000 cells. Three biological replicates were performed to achieve consistency. After complete cell attachment, 2 ml of DMEM was added to each well (6 h after inoculation) and the cells were then cultured for the next 7 days. The culture medium was changed on day 3 and 5. The growth of cells was evaluated using the 3-(4,5-dimethylthiazol-2-yl)-2,5-diphenyltetrazolium bromide (MTT) assay (21); blue formazan was dissolved in 2 ml of dimethylsulfoxide (DMSO; Sigma-Aldrich) and the absorbance of 200 μl of blue colored solution was measured at 570 nm using the microplate reader EL800 (Bio-Tek, Winooski, VT, USA). After the visualization of the cells by formazan production at the end of the MTT assay, photo-documentation was performed and the extension of single drops was acquired and analyzed using the graphical software ImageJ.

Migration of keratinocytes. For the migration test, neonatal keratinocytes (NKs) and adult keratinocytes (AKs) were used. Briefly, keratinocytes were inoculated at a density of 25,000 cells/cm^2 on the coverslips placed in an 8-well dish Nunc (Thermo Fisher Scientific, Rochester, NY, USA) on a mitomycin C-treated feeder layer (3T3 cells, 30,000 cells/cm^2) and further cultured in keratinocyte growth medium to full confluence. Uniform circular defects were made using the 8 mm biopsy punch (Kai Medical, Seki City, Japan). The size of single defects was photo-documented after 24, 48 and 96 h.

Table I. Antibodies used for immunocytochemical analysis.

Primary antibody	Supplier (location)	Secondary antibody/ fluorochrome	Supplier (location)
Wide spectrum cytokeratin/P	Abcam, Cambridge (Cambridge, UK)	Swine anti-rabbit/FITC	Dako (Glostrup, Denmark)
Cytokeratin 8/P Nestin/P Fibronectin/P	Sigma-Aldrich (Prague, Czech Republic)		
High molecular weight cytokeratin/M Cytokeratin 19/M Smooth muscle actin/M Vimentin/M	Dako (Glostrup, Denmark)	Goat anti-mouse/TRITC	Sigma-Aldrich (Prague, Czech Republic)
Cytokeratin 14/M	Sigma-Aldrich (Prague, Czech Republic)		

P, rabbit polyclonal; M, mouse monoclonal.

In parallel to decreasing the size of the defect, the phenotype of migrating keratinocytes was analyzed immunocytochemically.

Co-culture of fibroblasts and keratinocytes. Mutual interactions of fibroblasts and keratinocytes were studied in co-cultures using the insert system. The cells were always co-cultured in DMEM. To study the influence of keratinocytes on fibroblast migration, NFs or AFs were inoculated in the same manner as mentioned above. After their adhesion, collagen inserts (Corning) were placed into the wells and NKs or AKs were inoculated at a density of 40,000 cells/cm^2. Regarding the faster growth of fibroblasts influenced by keratinocytes, the experiment was evaluated by the MTT assay after 5 days. To study the influence of keratinocytes on fibroblast phenotype, NFs or AFs were inoculated on coverslips at a density of 1,000 cells/cm^2 and after adhesion, collagen inserts with AKs or NKs were placed into the wells. The cells were co-cultured for 7 days and the culture medium was changed every 2 days. Selected markers (vimentin, nestin, SMA and fibronectin) (Table I) were detected using immunocytochemistry. Finally, the influence of fibroblasts on keratinocyte phenotype was studied as well. NKs or AKs were seeded on coverslips, as described in the migration experiment and placed in 6-well plates. Twenty-four hours later, Falcon PET inserts (Corning) were put into the wells and AFs or NFs were inoculated at a density of 5,000 cells/insert. The cells were co-cultured under the same conditions as mentioned above. The phenotype of keratinocytes was detected by immunocytochemistry (keratin 8, 14 and 19) (Table I).

Immunocytochemistry (ICC). The cells grown on coverslips were fixed with 2% (w/v) paraformaldehyde in phosphate-buffered saline (PBS) for 10 min, then washed with PBS and permeabilized by 0.05% Triton X-100 (Sigma-Aldrich) in PBS. The non-specific binding of immunoglobulins via Fc receptors was blocked by 3.3% non-immune porcine serum (Dako, Glostrup, Denmark). The panel of antibodies used is presented in Table I (antibody dilution respected the supplier's instructions). The specificity of binding of the secondary antibodies was tested by isotype controls. Cell nuclei were counterstained with 4',6-diamidino-2-phenylindole (DAPI; Sigma-Aldrich). The stained coverslips were mounted in Vectashield (Vector Laboratories, Peterborough, UK) and analyzed using an Eclipse 90i fluorescence microscope (Nikon, Prague, Czech Republic) equipped with a Cool-1300Q CCD camera (Vosskühler GmbH, Osnabrück, Germany) and LUCIA 5.1 computer-assisted image analysis system (Laboratory Imaging, Prague, Czech Republic).

Polymerase chain reaction (PCR) analysis. RNA from subconfluent cultures of NFs and AFs was isolated using an RNeasy micro kit (Qiagen, Gaithersburg, MD, USA). DNase I (Qiagen) was applied in RNA solution to properly remove genomic DNA, and the purification procedure was repeated. Reverse transcription was performed with 1 μg of total RNA and an AccuScript High Fidelity First Strand cDNA Synthesis kit (Stratagene, San Diego, CA, USA) according to the manufacturer's instructions. For negative control, the same reverse transcription reaction without reverse transcriptase was performed. The PCR reaction was performed with REDTaq ReadyMix (Sigma-Aldrich). All primers are listed in Table II.

Transcriptome analysis. Total RNA was isolated using an RNeasy micro kit (Qiagen) according to the manufacturer's instructions. The quality and concentration of RNA were measured with a NanoDrop 2000 spectrophotometer (Thermo Fisher Scientific, Waltham, MA, USA). The RNA integrity was analyzed with an Agilent Bioanalyzer 2100 (Agilent, Santa Clara, CA, USA). Only samples with intact RNA profiles were used for expression profiling analyses (RIN >9).

Illumina HumanHT-12 v4 Expression BeadChips (Illumina, San Diego, CA, USA) were used for the microarray analysis following the standard protocol. In brief, 200 ng RNA was amplified with Illumina TotalPrep RNA Amplification kit (Ambion, Austin, TX, USA) and 750 ng of labeled RNA was hybridized

Table II. Primers for the genes of epidermal neural crest stem cell molecular signature.

Primer name	Sequence	Primer name	Sequence
Hs PCBP4_F	ctcctgcaaatggtggaaat	Hs GAPDH_R	tgtggtcatgagtccttcca
Hs PCBP4_R	ctgaccctggacagagaagc	Hs VARS2_F	gtctacctccatgccatcgt
Hs CALR_F	tctcagttccggcaagttct	Hs VARS2_R	gaagtggcggtaacccagta
Hs CALR_R	tctgagtctccgtgcatgtc	Hs CRMP1_F	ggcggtggagtacaacatct
Hs PYGO2_F	ctctgtcccaacgatttgct	Hs CRMP1_R	cacaggaccgtcatacatgc
Hs PYGO2_R	aagctgttggcatctggagt	Hs CRYAB_F	ttcttcggagagcacctgtt
Hs H1FX_F	gcgttgtccccatctaagaa	Hs CRYAB_R	ttttccatgcacctcaatca
Hs H1FX_R	agcttgaaggaaccgttgg	Hs MSX2_F	gtctccagcctgcccttc
Hs ETS 1_F	ggaggaccagtcgtggtaaa	Hs MSX2_R	gtggcatagagtcccacagg
Hs ETS 1_R	tttgaattcccagccatctc	Hs MYO10_F	cgcaacaaccaggatacctt
Hs PEG10_F	tcccactacctgatgcacaa	Hs MYO10_R	tccgcttctccagtttctgt
Hs PEG10_R	atctacctggtggtggcttg	Hs THOP1_F	agccttctgtgcatcgactt
Hs VDAC1_F	ctcagccaacactgagacca	Hs THOP1_R	tccttgaggatagcgcagtt
Hs VCAC1_R	cagccctcgtaacctagcac	Hs UBE4b_F	agcctctggtggagcaagta
Hs SELH_F	tagccgagaagcgagagaag	Hs UBE4b_R	ttaaggatttcggcaaccac
Hs SELH_R	gccccttcttaatcccagtc	Hs TSEN15_F	ggagatgccacccaagttta
Hs AGPAT6_F	gagtcctggaacctgctgag	Hs TSEN15_R	tggcagcataaatccatcag
Hs AGPAT6_R	gccaccatttcttggtctgt	Hs ADAM12_F	cagtttcacggaaacccact
Hs GAPGD_F	cgagatccctccaaaatcaa	Hs ADAM12_R	gcctctgaaactctcggttg

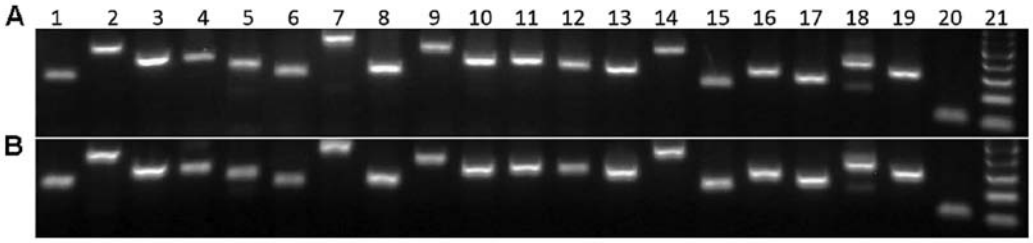

Figure 1. (A) Neonatal and (B) adult fibroblasts express markers of epidermal neural crest stem cells. 1, CRYAB; 2, PEG10; 3, AGPAT6; 4, UBE4B; 5, H1FX; 6, CRMP1; 7, MYO10; 8, SELH; 9, ETS1; 10, VDAC1, 11, TSEN15; 12, MSX2; 13, VARS2; 14, ADAM12; 15, CALR; 16, PYGO2; 17, THOP1; 18, PCBP4; 19, GAPDH; 20, 18S RNA; 21, 100 bp ladder.

on the chip according to the manufacturer's instructions. The analysis was performed in two biological replicates per group. The raw data were preprocessed using GenomeStudio software (version 1.9.0.24624; Illumina) and the limma package (22) of the Bioconductor (23), as previously described (24): the transcription profiles were background corrected using a normal-exponential model, quantile normalized and variance stabilized using base 2 logarithmic transformation.

The moderated t-test was used to detect transcripts differentially expressed between the sample groups [within limma; (21)]. False discovery rates values were used to select significantly differentially transcribed genes (FDR <0.05). The transcription data are Minimum Information About a Microarray Experiment (MIAME)-compliant and have been deposited in the ArrayExpress database. Gene set enrichment analysis (GSEA) and determination of gene functions were performed using Enrichr web service (25).

Statistical analysis. Statistical analysis was performed using PAST (version 3.12) free scientific analysis software kindly provided by Dr Ø. Hammer, University of Oslo, Norway. Individual data sets describing size of AF and NF covered areas were first tested for normality of distribution (Shapiro-Wilk test). To assess the equality of variances for both groups, Levene's test for homoscedasticity was used. Confirming these two assumptions, independent (two-tailed) t-test was performed to compare the size of AF- and NF-covered areas, respectively with the null hypothesis that the AF and NF covered areas are equal, alpha level 0.001. Thus, if the P-value is less than the chosen alpha level, then the null hypothesis is rejected and there is evidence that the data tested are unequal.

Results

Differentiation potential of NFs and AFs. Both NF as well as AF RNA profiles were consistent with the molecular signature of epidermal neural crest stem cells (26) (Fig. 1). However, these two cell types significantly differed in the differentiation potential. The adipogenic differentiation of NFs was confirmed by the adipocyte marker FABP4 (Fig. 2A) and

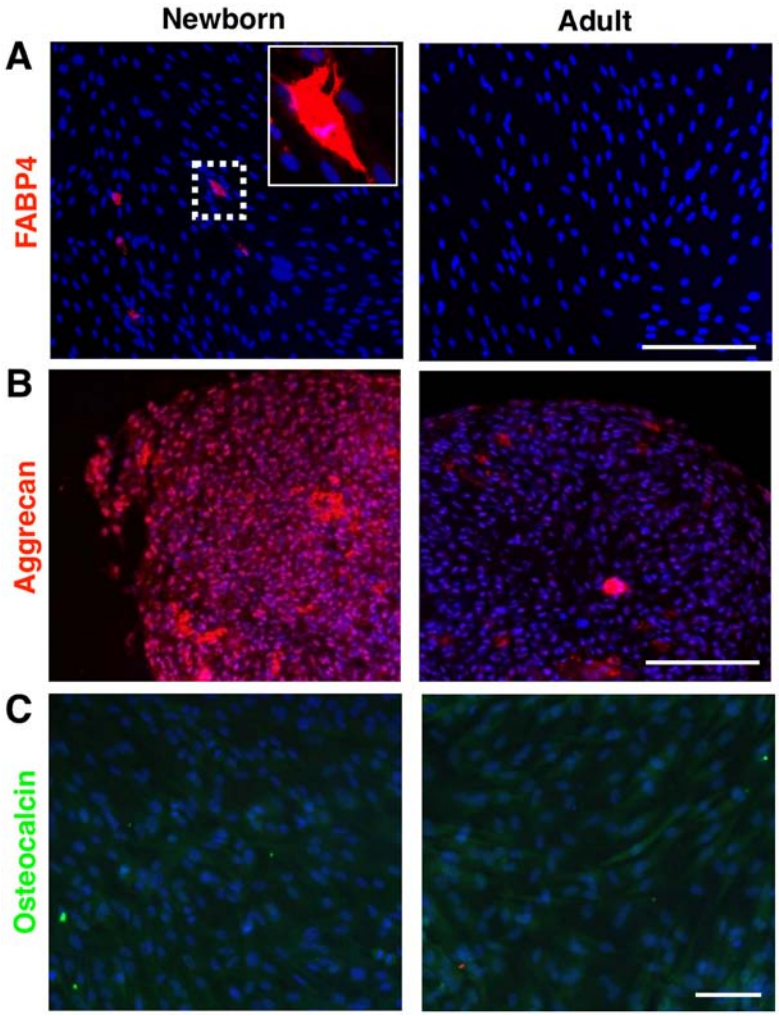

Figure 2. Plasticity of fibroblasts. Neonatal fibroblasts can be transformed to (A) adipocytes and (B) chondroblasts but not to (C) osteoblasts. FABP4 (red signal), aggrecan (red signal) and osteocalcin (green signal) were detected by immunofluorescence. Scale bar is 100 μm.

also by the content of lipid droplets (oil red positive staining, image not shown). Similarly, we succeeded in demonstrating the chondrogenic differentiation of NF (Fig. 2B), which was verified by the detection of aggrecan. However, we failed in the case of osteogenic differentiation in NFs (Fig. 2C). On the contrary, the adult counterparts (AFs) were not capable of differentiating into any of these three lineages (Fig. 2).

MTT assay and migration of fibroblasts. Surprisingly, the results of the MTT assay (Fig. 3A) indicated that the final metabolic activity of the NF and AF cultures were quite similar at the endpoint. When keratinocytes were added to the culture system, the growth of AFs as well as NFs increased approximately 1.7 times (as assessed by the MTT assay). Notable differences between the stimulation by NKs and AKs were not found (data not shown).

Cell migration was assessed on inoculum spreading visualized during the MTT assay at the same time. Regardless of the comparable metabolic activity of AFs and NFs, these cells differed in their migration potential. From the original 10 μl drop inoculum, AFs were able to reach the size of the final circular spot of 12 mm in diameter that was somewhat higher than in NFs (8.8 mm) (Fig. 3B and C). Both types of keratinocytes in Transwell co-culture further increased the migration of NFs in the same manner, while in AFs the situation remained the same. These results are clearly illustrated in Fig. 3D, where the space between the borders of neighboring growth is shown.

Migration of keratinocytes. The migration potential of NKs and AKs was studied on biopsy punch-made round defects (8 mm) in confluent monolayers of NKs and AKs, respectively. We observed remarkable differences between both keratinocyte types. NKs were able to heal the defect completely within 96 h (Fig. 4A) whereas nearly one third of the defect area in AKs remained unclosed at this time point (Fig. 4B). NKs colonizing the defect were uniformly very small (<5 μm), rounded and practically all cells expressed keratin 8. On the contrary, AKs created highly organized sheets and the very small keratinocytes were localized only at the leading edge. Moreover, all AKs were negative for keratin 8 (Fig. 4C).

Expression of αSMA and production of fibronectin. Both AFs as well as NFs produced fibronectin rich ECM and its production was further enhanced in co-cultures with keratinocytes. While NKs stimulated AFs and NFs to the same degree, AKs increased the production of fibronectin, mainly in NFs (Fig. 5). No MFs (αSMA-positive) were detected in AF cultures (Fig. 5A); however, numerous MFs were observed in

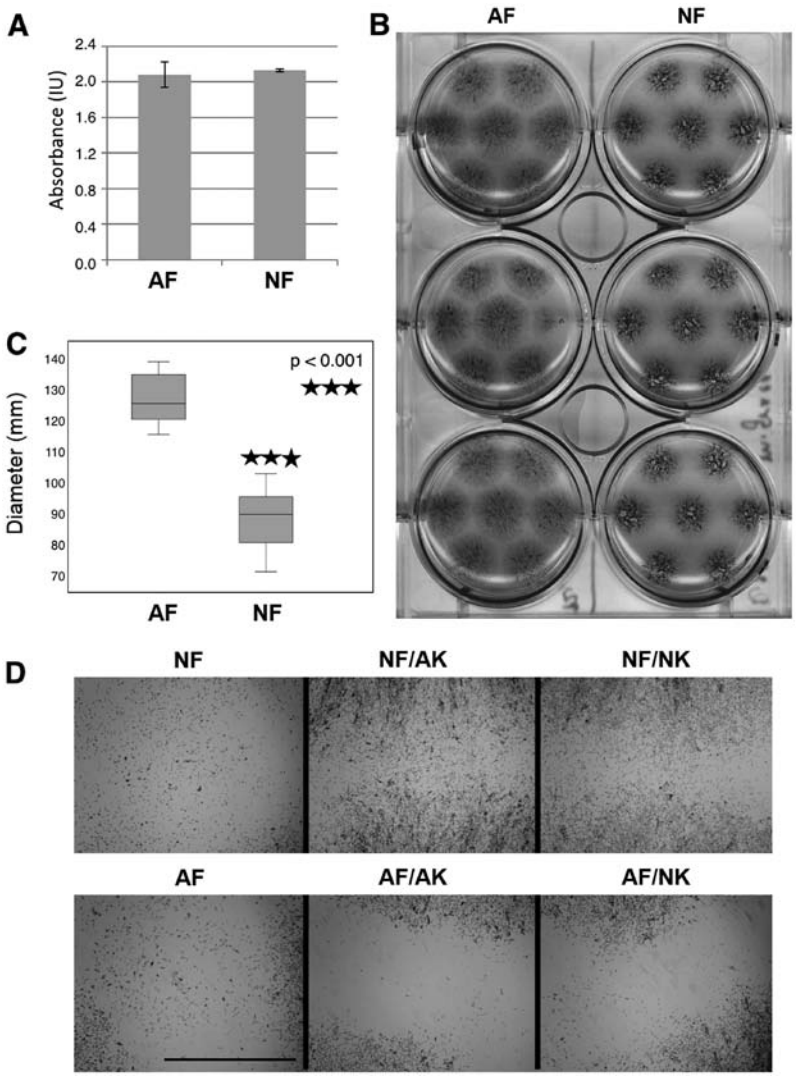

Figure 3. Proliferation and migration of fibroblasts. (A) No differences were found in the proliferation of neonatal fibroblasts (NFs) and adult fibroblasts (AFs) as measured by the MTT assay. (B) The migration of both cell types from microdrops significantly differed. While NFs remained more clustered, AFs migrated further from the original drop (MTT assay before the formazan dissolution). (C) At day 7 twenty clusters of each cell type (from 3 biological replicates) were used for the statistical evaluation. A statistically significant difference between AFs and NFs was found (P<0.001). (D) Adult keratinocytes (AKs) and newborn keratinocytes (NKs) did not differ in their effect on fibroblasts. While NFs influenced by keratinocytes increased their migration potential, in the case of AFs, it remained identical. MTT assay before the formazan dissolution, detail of the space between neighboring drops. Scale bar is 100 μm.

the case of NFs (Fig. 5B). The presence of AKs in co-culture resulted in a slight increase in the number of MFs in AF and NF cultures, respectively. By contrast, the presence of NKs in co-cultures generated a remarkable increment in the number of MFs in both AF and NF cultures, suggesting a higher frequency of transition to MFs (Fig. 5).

Expression of nestin. Nestin-positive fibroblasts were very rare in the culture of normal AFs (Fig. 6A). Strikingly, the majority of NFs were positive for this intermediate filament (Fig. 6B). Both AKs and NKs in co-culture stimulated the expression of nestin in both AF and NF cultures (Fig. 6). While the increase in nestin positivity was uniformly distributed over the population of AFs (Fig. 6A), the nestin-positive NFs were detected only locally in the case of AKs (Fig. 6B).

ICC of co-cultures of keratinocytes and fibroblasts (AF/AK, AF/NK, NF/NK and NF/AK). At day 7, individual keratinocyte colonies were still isolated in all experimental settings. Small keratinocytes were present at their peripheries. In the co-culture of NFs with NKs (NF/NK), small keratinocytes frequently expressed keratin 8 and 19 (image not shown). Furthermore all cells were positive for keratin 14. The occurrence of small, rounded keratinocytes on the periphery of colonies was significantly rarer when NKs were cultured with AFs (Fig. 7A) and the expression of the keratins studied in NKs decreased. Strikingly, NFs strongly influenced the phenotype of AKs (Fig. 7B). This NF/AK experimental setting typically resulted in a significantly higher number of small keratinocytes exhibiting triple positivity K8/19/14 than seen in co-cultures of AF/AK (image not shown) and even in co-cultures of AF/NK (Fig. 7). These small keratinocytes in AK/NF type co-cultures were devoid of typical intercellular bridges.

Comparison of expression profiles of NFs and AFs fibroblasts. In this study using microarray technology expression profiles

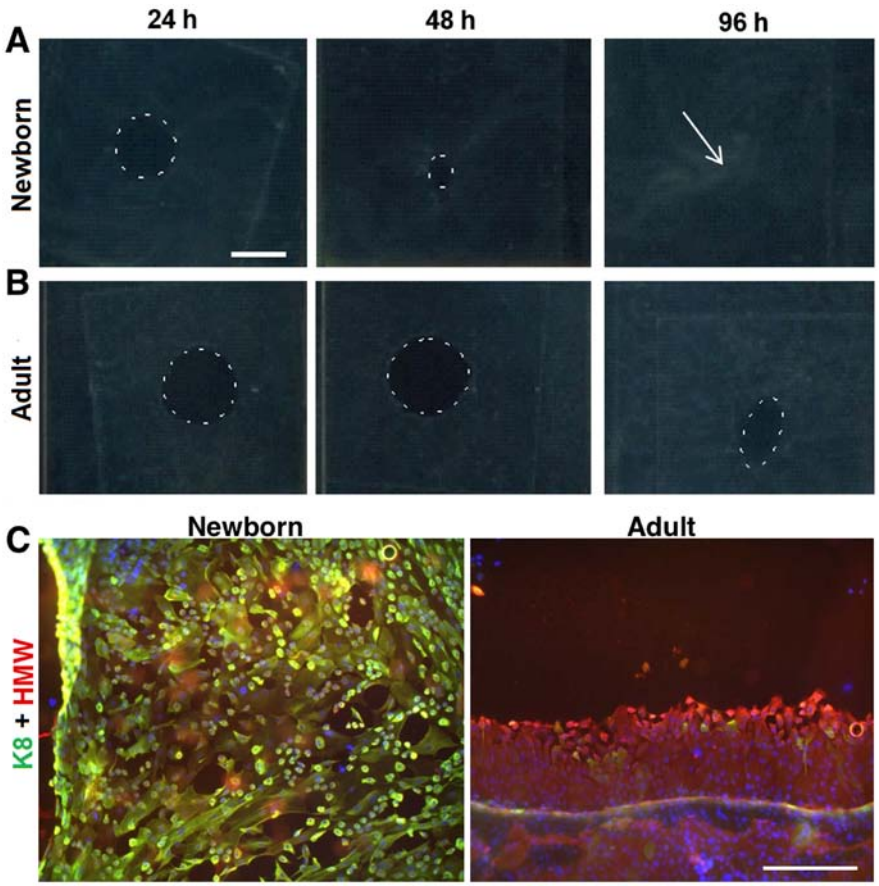

Figure 4. Closure of defect by keratinocytes. (A) Neonatal keratinocytes (NKs, newborn) closed the standard defect in culture at the stage of confluent growth faster than (B) adult keratinocytes (AKs, adult). (C) Numerous small NKs positive for keratin 8 (K8; green signal) form a thick border closing the defect after 24 h. The border of the defect is very tight and the number of K8-positive cells is highly limited in the case of AKs. The cells were stained with high molecular weight keratin (red signal) and K8. Scale bar is 8 mm (A and B) and 100 μm (C).

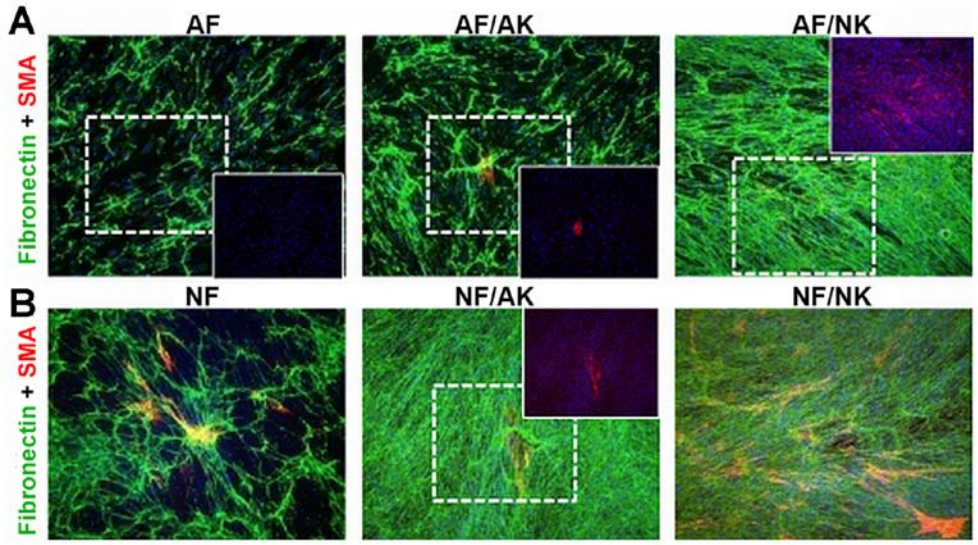

Figure 5. Transition of fibroblasts to myofibroblasts. (A) The culture of adult fibroblasts (AFs) was negative for the presence of myofibroblasts exhibiting α-smooth muscle actin [SMA, red signal]. Adult keratinocytes (AKs) as well as neonatal keratinocytes (NKs) stimulated the transition of AFs to myofibroblasts. (B) The culture of neonatal fibroblasts (NFs) exhibited the presence of myofibroblasts. Their incidence was stimulated by NKs only (B). Both types of fibroblasts produced fibronectin [(A and B) green signal]. AKs and NKs stimulated the production of this structural molecule of the extracellular matrix. Scale bar is 100 μm.

of cultivated NFs and AFs were compared. Interestingly, the expression analysis revealed the existence of 1,509 differentially-regulated genes (FDR <0.05).

Growth factors, ILs and other extracellular factors, together with ECM-related genes were considered the most important group of genes with the potential to influence the investigated

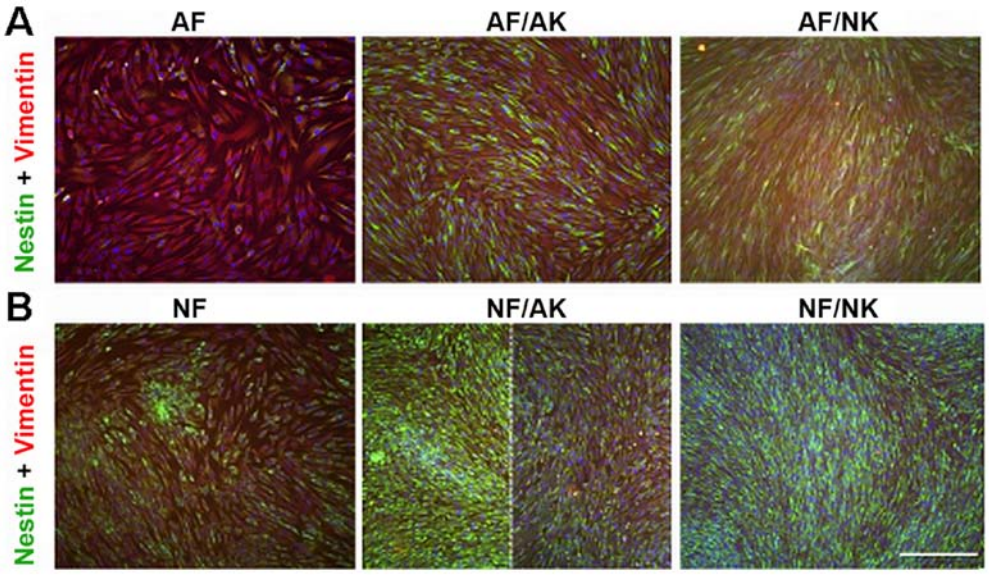

Figure 6. Expression of nestin in fibroblasts under different conditions. (A) Adult fibroblasts (AFs) were positive for vimentin [red signal] and negative for nestin [green signal]. Both neonatal keratinocytes (NKs) as well as adult keratinocytes (AKs) stimulated the expression of nestin in AFs. (B) Neonatal fibroblasts (NFs) were positive for vimentin and nestin. While NKs had a stimulatory effect on all NFs, AKs stimulated the expression of nestin in NFs only locally. It is documented on two different places of one glass separated by white dotted line. Scale bar is 100 μm.

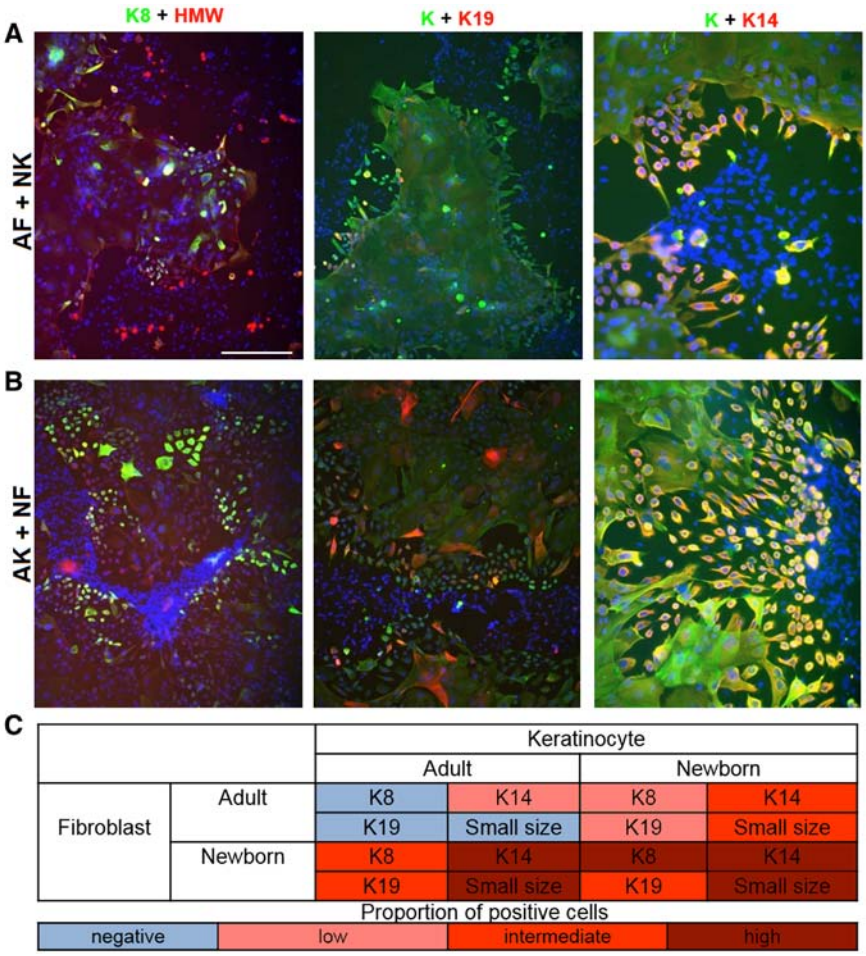

Figure 7. Influence of the age of fibroblasts on the phenotype of keratinocytes. (A) Adult fibroblasts (AFs) had a negative effect on the incidence of small neonatal keratinocytes (NKs) located on peripheries of compact colonies positive for keratin 8 (K8; green signal), keratin 19 (K19; red signal) and keratin 14 (K14; red signal). HMW represents high molecular weight cytokeratin and K wide spectrum cytokeratin. The nuclei of the cells were visualized with DAPI (blue color). (B) Neonatal fibroblasts (NFs) had a strong stimulatory effect on the occurrence of small adult keratinocytes (AKs) positive for the above-mentioned keratins. Scale bar is 100 μm. (C) Obtained phenotype of keratinocytes is summarized schematically; blue color represents lacking of the markers of low maturation (small size, K8, K19) and so high differentiation status of keratinocytes with this phenotype. Increasing intensity of red hue correlates with the higher incidence of these markers and so with decreasing maturation of keratinocytes.

Table III. GSEA (GO Biological processes) of the group of extracellular factors upregulated in NFs (FDR <0.2).

Term	Overlap	P-value	Adjusted P-value	Z-score	Combined score
Positive regulation of cell division (GO:0051781)	9/120	2.5E-10	3.1E-07	-2.25	33.67
Positive regulation of MAPK cascade (GO:0043410)	12/395	3.9E-09	1.7E-06	-2.46	32.72
Regulation of cell division (GO:0051302)	10/234	4.1E-09	1.7E-06	-2.39	31.75
Growth (GO:0040007)	10/329	9.3E-08	1.9E-05	-2.41	26.11
Regulation of cell growth (GO:0001558)	10/322	7.7E-08	1.9E-05	-2.34	25.42
Cell chemotaxis (GO:0060326)	8/155	4.3E-08	1.3E-05	-2.25	25.24
Chemotaxis (GO:0006935)	9/263	1.7E-07	2.6E-05	-2.39	25.18
Taxis (GO:0042330)	9/263	1.7E-07	2.6E-05	-2.39	25.16
Positive regulation of peptidyl-tyrosine phosphorylation (GO:0050731)	7/139	3.8E-07	5.0E-05	-2.27	22.48
Response to corticosteroid (GO:0031960)	7/140	4.0E-07	5.0E-05	-2.24	22.20

GSEA, gene set enrichment analysis; NFs, neonatal fibroblasts.

phenotype of cells. Thus, we performed GSEA of the group of extracellular factors upregulated in NFs (FDR <0.2) with the aim of determining their specific biological role and prospective agents that may be responsible for paracrine stimulation. The following genes from those upregulated in NFs are known to positively regulate cell division (GO:0051781: FGF5, TGFB2, MDK, TGFB3, IL1B, VEGFB, FGF1, PGF and VEGFA), cell growth (GO:0001558: TGFB2, IGFBP5, IGFBP4, IGFBP2, IGFBP7, NGF, KAZALD1, CTGF, CXCL16, VEGFA, GDF10, IL-6, TGFB3, INHBB, FGF1 and BMP6) and stimulate cell chemotaxis (GO:0060326: CXCL6, TGFB2, IL-6, IL1B, VEGFB, CXCL1, CXCL14, CXCL16 and VEGFA). Arguably, the observed differences in the expression of genes, which stimulate cells responsible for the acute phase of the inflammatory response, could be the reason why stimulation by NFs improves tissue regeneration (Table III).

Overall, NFs and AF differ in the expression of genes that influence ECM organization (GO:0030198 and GO:0022617), morphogenesis (GO:0009887 and GO:0048598), cell adhesion (GO:0030155), epithelial cell proliferation (GO:0050678), angiogenesis (GO:0001525) and ossification (GO:0030278), as well as positively regulate cell motility and migration (GO:2000147 and GO:0030335) (see Table IV for full details). The products of the deregulated genes localize primarily to the ECM (GO:0031012), extracellular space (GO:0005615), and cell surface (GO:0009986). The changes also occur in adherent (GO:0005912) and anchoring junctions (GO:0070161). From the molecular function perspective, these products are mainly responsible for binding of glycosaminoglycans (GO:0005539), sulfur compounds (GO:1901681), collagen (GO:0005518), heparin (GO:0008201), IGF (GO:0005520), cell adhesion molecules (GO:0050839) as well as ECM structural constitution (GO:0005201), growth factor activity (GO:0008083) and many other functions related to extracellular processes.

Discussion

This study illustrates significant functional and morphological differences between adult and newborn fibroblasts and keratinocytes and thus harmonizes with our previous observations (6). In this context, NFs express nestin and they are also frequently positive for αSMA. This makes them distinct from AFs. Nestin-positive fibroblasts were also described *in vivo* in fetal human skin (27). Our successful *in vitro* differentiation of NFs into adipocytes and chondrocytes is in agreement with similar observations reported by others (28). This remarkable plasticity of NFs is later lost during life and thus, not seen in AFs. The high frequency of spontaneous transformation of NFs to MFs is most likely related to wound contraction, a key step of proper wound closure (14). Besides this, NKs were able to heal standardized experimental *in vitro* wounds in a significantly shorter time than AKs. When we focused on the fibroblast-keratinocyte interactions in the co-culture, NFs (not seen in the co-culture with AFs) induced the presence of numerous small keratinocytes on the periphery of the AK colonies. These small peripheral AKs lacked intercellular contacts and all were positive for keratin 14 (marker of basal layer), K8 and K19 (markers of simple epithelia), thus indicating the poor differentiation level of the cells (29). Of note, keratin 19 is present in the fetal epidermis, but not in adult interfollicular epidermal keratinocytes (30). Keratin 8 is typically paired with keratin 18 and is temporarily present in the developing epidermis and malignant tumors (31). Furthermore, these small keratinocytes were observed earlier in fetal/neonatal epidermis of human and porcine origin, respectively (6,32). Fibroblasts isolated from epidermal carcinomas and dermatofibroma revealed a similar effect to AKs in the co-culture (17,19,33). Similarly, melanoma cells and neural crest stem cells isolated from hair follicles induced the presence of small cells at the periphery of AK colonies (34). The seemingly malignant phenotype of these small keratinocytes does not imply that the cells underwent malignant transformation. Interestingly, these experiments revealed remarkable similarities between wound repair and tumor growth as already postulated by Dvorak and later by other authors (13,35,36).

As elucidated elsewhere (19), even on the protein level it has been shown that pro-inflammatory factors such as IL-6, IL-8 and CXCL1, produced by CAFs, influence the phenotype of keratinocytes. Although the effector molecules acting on epidermal cells are similar in the case of CAFs and NF, the final effect is not identical. NFs differ from AFs in the expression

Table IV. GSEA (GO terms) of the genes deregulated between NFs and AFs (FDR <0.05).

Term	Overlap	P-value	Adjusted P-value	Z-score	Combined score
GO: Biological processes					
Extracellular matrix organization (GO:0030198)	91/359	2.6E-18	6.7E-15	-2.38	77.69
Extracellular structure organization (GO:0043062)	91/360	3.0E-18	6.7E-15	-2.38	77.68
Organ morphogenesis (GO:0009887)	79/405	6.0E-11	9.0E-08	-2.36	38.26
Embryonic morphogenesis (GO:0048598)	76/403	5.4E-10	6.1E-07	-2.43	34.73
Regulation of cell adhesion (GO:0030155)	66/336	1.9E-09	1.7E-06	-2.45	32.62
Regulation of epithelial cell proliferation (GO:0050678)	53/258	2.1E-08	1.2E-05	-2.45	27.83
Angiogenesis (GO:0001525)	51/236	9.2E-09	6.9E-06	-2.30	27.33
Embryonic organ morphogenesis (GO:0048562)	34/121	1.4E-08	9.1E-06	-2.19	25.48
Positive regulation of cell motility (GO:2000147)	54/287	1.9E-07	6.6E-05	-2.46	23.67
Positive regulation of cell migration (GO:0030335)	53/280	2.1E-07	6.7E-05	-2.45	23.58
GO: Cellular component					
Extracellular matrix (GO:0031012)	90/348	1.8E-18	8.9E-16	-2.25	78.03
Extracellular space (GO:0005615)	163/1120	2.3E-11	5.6E-09	-2.19	41.63
Extracellular matrix part (GO:0044420)	37/127	1.7E-09	2.7E-07	-2.12	31.97
Proteinaceous extracellular matrix (GO:0005578)	53/239	2.6E-09	3.2E-07	-2.12	31.64
Cell surface (GO:0009986)	72/437	2.4E-07	2.4E-05	-2.25	23.95
Extracellular region (GO:0005576)	183/1585	7.2E-06	2.9E-04	-2.43	19.80
Adherens junction (GO:0005912)	64/405	3.9E-06	2.7E-04	-2.25	18.47
Anchoring junction (GO:0070161)	65/419	5.6E-06	2.8E-04	-2.22	18.14
Cell-substrate adherens junction (GO:0005924)	58/358	5.7E-06	2.8E-04	-2.21	18.06
Extracellular vesicular exosome (GO:0070062)	291/2717	2.9E-06	2.4E-04	-2.15	17.93
GO: Molecular function					
Glycosaminoglycan binding (GO:0005539)	40/190	4.9E-07	1.7E-04	-2.36	20.55
Sulfur compound binding (GO:1901681)	42/206	5.4E-07	1.7E-04	-2.32	20.16
Extracellular matrix structural constituent (GO:0005201)	23/68	1.7E-07	1.6E-04	-2.22	19.40
Collagen binding (GO:0005518)	20/62	2.0E-06	4.6E-04	-2.22	17.05
Growth factor activity (GO:0008083)	33/163	9.9E-06	1.5E-03	-2.34	15.18
Heparin binding (GO:0008201)	30/140	9.6E-06	1.5E-03	-2.23	14.45
Insulin-like growth factor binding (GO:0005520)	11/27	7.6E-05	8.7E-03	-2.95	13.97
Cell adhesion molecule binding (GO:0050839)	32/168	3.8E-05	5.0E-03	-2.29	12.11
Fibronectin binding (GO:0001968)	10/26	2.3E-04	1.8E-02	-2.78	11.16
RNA polymerase II core promoter proximal region sequence-specific DNA binding transcription factor activity (GO:0000982)	35/204	1.1E-04	1.0E-02	-2.29	10.53

GSEA, gene set enrichment analysis; NFs, neonatal fibroblasts, AFs, adult fibroblasts.

of several genes related to ECM structure and organization. However, both types of fibroblasts (NFs and AFs) produce selected structural glycoproteins, e.g. fibronectin, to a comparable extent. However, the genome-wide analysis also revealed differentially-expressed genes positively regulating cell division and proliferation, and genes for chemotaxis. The products of upregulated chemotactic genes, such as IL1B, IL-6, CXCL1, CXCL6, CXCL14, CXCL16, TGFB2, VEGFA and VEGFB, are involved in the acute phase of the inflammatory response. The observed differences in their expression herein, may also be responsible for remarkably efficient wound healing in the short postnatal period. Indeed, inflammation during the course of prenatal and neonatal healing is attenuated with diminished production of IL-6, IL-8 and CXCL1 by NFs (37). In this study, we also found 51 differentially-regulated genes associated with angiogenesis, a process that is of utmost importance to wound healing. Taken together, these data suggest that a large number of expressed genes involved in tissue repair and regeneration differ between AFs and NFs. Clarifying differences in the expression profiles of NFs and AFs will allow us to better understand the excellent results of lip cleft surgery in neonates reported by clinicians (5).

However, at this point in time it still remains speculative whether the course of ageing reflects the difference between

neonatal and adult cells. Therefore, we can only hypothesize whether the mechanism is genetic or epigenetic. The moment of birth represents a sharp threshold requiring prompt adaptation of the newborn organism to exist independently from the maternal body in the outer environment. However, clinical evidence demonstrates that the improved and almost scarless prenatal healing in mammals (including humans) persists also during the early postnatal period of life (38,39). The age of the cell donor thus represents a very important parameter influencing the behavior of cells *in vitro* and it also affects the course of wound healing after grafting. An observed antifibrotic effect of NFs (40) as well as expression profiles of human fibroblasts performed by us and others (41) support these findings.

We conclude that phenotype and functional properties, including EMI, of NFs and NKs differ from those seen in adult cells. These differences can, in addition to other factors, participate in the successful and almost scarless healing during the neonatal period. From this point of view, this study brings new data demonstrating the functional consequences that can help us to better understand the molecular basis of differences between neonatal and adult wound healing. Further studies deciphering particular mechanisms responsible for these differences are needed, because this knowledge may be of great clinical significance in wound healing management.

Acknowledgements

The authors are grateful to Marie Jindráková and Radana Kavková for excellent technical assistance. This study was supported by the Grant Agency of the Czech Republic (P304-13-20293S), the Charles University (project of Specific University Research, PRVOUK-27 and UNCE 204013) and by LQ1604 NPU II provided by MEYS and CZ.1.05/1.1.00/02.0109 BIOCEV provided by ERDF and MEYS. This publication is also in part a result of the project implementation: 'The Equipment for Metabolomic and Cell Analyses' (no. CZ.1.05/2.1.00/19.0400, supported by the Research and Development for Innovations Operational Programme (RDIOP) co-financed by the European Regional Development Fund and the state budget of the Czech Republic). The fellowship of Rosana Mateu in Prague was supported by Marie Curie Training Network project GLYCOPHARM (contract no. 317297). The study was also supported in part by the Agency for Science and Research (APVV-14-0731 and APVV-0408-12) and the Grant Agency of the Ministry of Education, Science, Research and Sport of the Slovak Republic (VEGA-1/0404/15 and VEGA-1/0048/15). The authors are also grateful to Dr Ø. Hammer and co-workers (42) for PAST for free access to statistical software package.

References

1. Liechty KW, Adzick NS and Crombleholme TM: Diminished interleukin 6 (IL-6) production during scarless human fetal wound repair. Cytokine 12: 671-676, 2000.
2. Bukovsky A, Caudle MR, Carson RJ, Gaytán F, Huleihel M, Kruse A, Schatten H and Telleria CM: Immune physiology in tissue regeneration and aging, tumor growth, and regenerative medicine. Aging (Albany NY) 1: 157-181, 2009.
3. Walraven M, Talhout W, Beelen RH, van Egmond M and Ulrich MM: Healthy human second-trimester fetal skin is deficient in leukocytes and associated homing chemokines. Wound Repair Regen 24: 533-541, 2016.
4. Han M, Yang X, Lee J, Allan CH and Muneoka K: Development and regeneration of the neonatal digit tip in mice. Dev Biol 315: 125-135, 2008.
5. Borsky J, Veleminska J, Jurovčík M, Kozak J, Hechtova D, Tvrdek M, Cerny M, Kabelka Z, Fajstavr J, Janota J, *et al*: Successful early neonatal repair of cleft lip within first 8 days of life. Int J Pediatr Otorhinolaryngol 76: 1616-1626, 2012.
6. Krejčí E, Kodet O, Szabo P, Borský J, Smetana K Jr, Grim M and Dvořánková B: In vitro differences of neonatal and later postnatal keratinocytes and dermal fibroblasts. Physiol Res 64: 561-569, 2015.
7. Yamaguchi Y, Itami S, Tarutani M, Hosokawa K, Miura H and Yoshikawa K: Regulation of keratin 9 in nonpalmoplantar keratinocytes by palmoplantar fibroblasts through epithelial-mesenchymal interactions. J Invest Dermatol 112: 483-488, 1999.
8. Biggs LC and Mikkola ML: Early inductive events in ectodermal appendage morphogenesis. Semin Cell Dev Biol 25-26: 11-21, 2014.
9. Mikkola ML and Millar SE: The mammary bud as a skin appendage: unique and shared aspects of development. J Mammary Gland Biol Neoplasia 11: 187-203, 2006.
10. Rawles ME: Tissue interactions in scale and feather development as studied in dermal-epidermal recombinations. J Embryol Exp Morphol 11: 765-789, 1963.
11. Cohen BH, Lewis LA and Resnik SS: Would healing: a brief review. Int J Dermatol 14: 722-726, 1975.
12. Kwon YB, Kim HW, Roh DH, Yoon SY, Baek RM, Kim JY, Kweon H, Lee KG, Park YH and Lee JH: Topical application of epidermal growth factor accelerates wound healing by myofibroblast proliferation and collagen synthesis in rat. J Vet Sci 7: 105-109, 2006.
13. Smetana K Jr, Szabo P, Gál P, André S, Gabius HJ, Kodet O and Dvořánková B: Emerging role of tissue lectins as microenvironmental effectors in tumors and wounds. Histol Histopathol 30: 293-309, 2015.
14. Dvořánková B, Szabo P, Lacina L, Gal P, Uhrova J, Zima T, Kaltner H, André S, Gabius HJ, Sykova E and Smetana K Jr: Human galectins induce conversion of dermal fibroblasts into myofibroblasts and production of extracellular matrix: potential application in tissue engineering and wound repair. Cells Tissues Organs 194: 469-480, 2011.
15. Smetana K Jr, Dvořánková B, Szabo P, Strnad H and Koláø M: Role of stromal fibroblasts in cancer originated from squamous epithelia. In: Dermal Fibroblasts: Histological Perspectives, Characterization and Role in Disease. Bai X (ed). Nova Sciences Publishers, New York, pp83-94, 2013.
16. Strnad H, Lacina L, Kolár M, Cada Z, Vlcek C, Dvoránková B, Betka J, Plzák J, Chovanec M, Sáchová J, *et al*: Head and neck squamous cancer stromal fibroblasts produce growth factors influencing phenotype of normal human keratinocytes. Histochem Cell Biol 133: 201-211, 2010.
17. Lacina L, Smetana K Jr, Dvoránková B, Pytlík R, Kideryová L, Kucerová L, Plzáková Z, Stork J, Gabius HJ and André S: Stromal fibroblasts from basal cell carcinoma affect phenotype of normal keratinocytes. Br J Dermatol 156: 819-829, 2007.
18. Lacina L, Dvoránkova B, Smetana K Jr, Chovanec M, Plzák J, Tachezy R, Kideryová L, Kucerová L, Cada Z, Boucek J, *et al*: Marker profiling of normal keratinocytes identifies the stroma from squamous cell carcinoma of the oral cavity as a modulatory microenvironment in co-culture. Int J Radiat Biol 83: 837-848, 2007.
19. Kolář M, Szabo P, Dvořánková B, Lacina L, Gabius HJ, Strnad H, Sáchová J, Vlček C, Plzák J, Chovanec M, *et al*: Upregulation of IL-6, IL-8 and CXCL-1 production in dermal fibroblasts by normal/malignant epithelial cells in vitro: immunohistochemical and transcriptomic analyses. Biol Cell 104: 738-751, 2012.
20. Szabo P, Valach J, Smetana K Jr and Dvořánková B: Comparative analysis of production of IL-8 and CXCL-1 by normal and cancer stromal fibroblasts. Folia Biol 59: 134-147, 2013.
21. Ferrari M, Fornasiero MC and Isetta AM: MTT colorimetric assay for testing macrophage cytotoxic activity in vitro. J Immunol Methods 131: 165-172, 1990.
22. Smyth GK: Linear models and empirical Bayes methods for assessing differential expression in microarray experiments. Stat Appl Genet Mol Biol 3: e3, 2004.
23. Gentleman RC, Carey VJ, Bates DM, Bolstad B, Dettling M, Dudoit S, Ellis B, Gautier L, Ge Y, Gentry J, *et al*: Bioconductor: open software development for computational biology and bioinformatics. Genome Biol 5: R80, 2004.

24. Valach J, Fík Z, Strnad H, Chovanec M, Plzák J, Cada Z, Szabo P, Sáchová J, Hroudová M, Urbanová M, *et al*: Smooth muscle actin-expressing stromal fibroblasts in head and neck squamous cell carcinoma: increased expression of galectin-1 and induction of poor prognosis factors. Int J Cancer 131: 2499-2508, 2012.
25. Chen EY, Tan CM, Kou Y, Duan Q, Wang Z, Meirelles GV, Clark NR and Ma'ayan A: Enrichr: interactive and collaborative HTML5 gene list enrichment analysis tool. BMC Bioinformatics 14: 128, 2013.
26. Hu YF, Zhang ZJ and Sieber-Blum M: An epidermal neural crest stem cell (EPI-NCSC) molecular signature. Stem Cells 24: 2692-702, 2006.
27. Sellheyer K and Krahl D: Spatiotemporal expression pattern of neuroepithelial stem cell marker nestin suggests a role in dermal homeostasis, neovasculogenesis, and tumor stroma development: a study on embryonic and adult human skin. J Am Acad Dermatol 63: 93-113, 2010.
28. Chang Y, Guo K, Li Q, Li C, Guo Z and Li H: Multiple directional differentiation difference of neonatal rat fibroblasts from six organs. Cell Physiol Biochem 39: 157-171, 2016.
29. Lane EB and McLean WH: Keratins and skin disorders. J Pathol 204: 355-366, 2004.
30. Tan KK, Salgado G, Connolly JE, Chan JK and Lane EB: Characterization of fetal keratinocytes, showing enhanced stem cell-like properties: a potential source of cells for skin reconstruction. Stem Cell Rep 3: 324-338, 2014.
31. Casanova ML, Bravo A, Martínez-Palacio J, Fernández-Aceñero MJ, Villanueva C, Larcher F, Conti CJ and Jorcano JL: Epidermal abnormalities and increased malignancy of skin tumors in human epidermal keratin 8-expressing transgenic mice. FASEB J 18: 1556-1558, 2004.
32. Klíma J, Motlík J, Gabius H-J and Smetana K Jr: Phenotypic characterization of porcine interfollicular keratinocytes separated by elutriation: a technical note. Folia Biol (Praha) 53: 33-36, 2007.
33. Kideryová L, Lacina L, Dvoránková B, Stork J, Cada Z, Szabo P, André S, Kaltner H, Gabius HJ and Smetana K Jr: Phenotypic characterization of human keratinocytes in coculture reveals differential effects of fibroblasts from benign fibrous histiocytoma (dermatofibroma) as compared to cells from its malignant form and to normal fibroblasts. J Dermatol Sci 55: 18-26, 2009.
34. Kodet O, Lacina L, Krejčí E, Dvořánková B, Grim M, Štork J, Kodetová D, Vlček Č, Šáchová J, Kolář M, *et al*: Melanoma cells influence the differentiation pattern of human epidermal keratinocytes. Mol Cancer 14: 1, 2015.
35. Dvorak HF: Tumors: Wounds that do not heal. Similarities between tumor stroma generation and wound healing. N Engl J Med 315: 1650-1659, 1986.
36. Lacina L, Plzak J, Kodet O, Szabo P, Chovanec M, Dvorankova B and Smetana K Jr: Cancer microenvironment: what can we learn from the stem cell niche. Int J Mol Sci 16: 24094-24110, 2015.
37. Bermudez DM, Canning DA and Liechty KW: Age and pro-inflammatory cytokine production: wound-healing implications for scar-formation and the timing of genital surgery in boys. J Pediatr Urol 7: 324-331, 2011.
38. Muneoka K, Allan CH, Yang X, Lee J and Han M: Mammalian regeneration and regenerative medicine. Birth Defects Res C Embryo Today 84: 265-280, 2008.
39. Choi Y, Cox C, Lally K and Li Y: The strategy and method in modulating finger regeneration. Regen Med 9: 231-242, 2014.
40. Pratsinis H, Armatas A, Dimozi A, Lefaki M, Vassiliu P and Kletsas D: Paracrine anti-fibrotic effects of neonatal cells and living cell constructs on young and senescent human dermal fibroblasts. Wound Repair Regen 21: 842-851, 2013.
41. Kalfalah F, Seggewiß S, Walter R, Tigges J, Moreno-Villanueva M, Bürkle A, Ohse S, Busch H, Boerries M, Hildebrandt B, *et al*: Structural chromosome abnormalities, increased DNA strand breaks and DNA strand break repair deficiency in dermal fibroblasts from old female human donors. Aging (Albany NY) 7: 110-122, 2015.
42. Hammer Ø, Harper DAT and Ryan PD: PAST: Paleontological statistics software package for education and data analysis. Palaeontol Electronica 4: 9pp, 2001.